Asian Journal of Chemistry; Vol. 32, No. 11 (2020), 2927-2933

ASIAN JOURNAL OF CHEMISTRY

https://doi.org/10.14233/ajchem.2020.22901

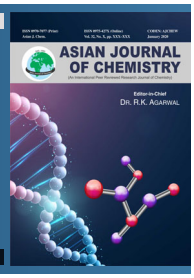

Synthesis and Characterization of Mesoporous Silica Carrier Releasing Valsartan

F. MUHANA[1,*], R. ABU-HUWAIJ[2], N. KHALAF[3], F. KHALILI[4] and N. SHALAN[2]

[1]Department of Pharmaceutical Science, Al-Ahliyya Amman University, Al-Salt, Jordan
[2]Pharmacological & Diagnostic Research Center, Faculty of Pharmacy, Department of Pharmaceutics & Pharmaceutical Technology, Al-Ahliyya Amman University, Al-Salt, Jordan
[3]Pharmacological & Diagnostic Research Center, Faculty of Pharmacy, Department of Pharmaceutical Sciences, Al-Ahliyya Amman University, Al-Salt, Jordan
[4]Faculty of Science, Department of Chemistry, University of Jordan, Amman, Jordan

*Corresponding author: Fax: + 96 26 5333315; Tel: + 98 25 3500211; E-mail: f.muhana@ammanu.edu.jo; Fhmuhana@gmail.com

Received: 14 July 2020; *Accepted*: 29 September 2020; *Published online*: 28 October 2020; AJC-20119

The aim of the present study is to synthesize a mesoporous silica MCM-48 and loading it with the poorly soluble drug valsartan. The MCM-48 was characterized by Brauner-Emmett-Teller surface area analyzer, scanning electron microscope, powder X-ray diffraction, thermal gravimetric analysis and Fourier transform infra-red (FTIR). The exact loading capacity was found to be 40.12%. *in vitro* dissolution studies at physiological conditions demonstrated controlled release of 57.2% valsartan over 240 min. The controlled dissolution was attributed to the incomplete amorphization of crystalline valsartan by MCM-48 as evidenced by PXRD studies. The interactions between the mesoporous silica surface and drug molecules were evidenced by FTIR studies and the diffusion of therapeutic agent molecules through the silica pores. The results of the present study confirmed that the controlled adsorption and liberation of valsartan demonstrated a long-term release, which is important for its antihypertensive activity. Moreover, the structural properties of mesoporous silica assured the feasibility of designing reliable drug delivery systems by appropriate choice of the carrier.

Keywords: Mesoporous, MCM-48, Mesoporous silica, Valsartan, Low water solubility, Antihypertensive, Drug delivery.

INTRODUCTION

In view of the great challenges to solve the problem of incomplete drug absorption across the gastrointestinal tract of the poorly water soluble drugs, inorganic mesoporous silicates materials exceled to be critically important to reach a progress in superior drug development. They are a promising class of synthetic polymers, widely used in catalysis of reactions [1] drug delivery and adsorbents for toxicants [2]. Mesoporous silicate materials have excellent many attractive physico-chemical characteristics, such as large surface and pore volume, which permits the binding of different functional groups for targeted the drug entity, with tunable pore sizes. These materials have openedthe framework pore structure [3], thermal and chemical stability, cheap, safe, hydrophilic and easily synthesizable [4]. Moreover, they have enriched surface silanol groups and easy surface modifications [5] to expand its scope of applications. In addition, studies have shown that mesoporous silica materials have good biocompatibility and biodegradability in animal and plant cells [6].

MCM-48 is a mesoporous silicate material consisting 3D channel topology structure with cubic space and contains two independent intertwined networks of channels. These properties make MCM-48 very attractive for developing systems aiming to release drugs in a controlled manner. The presence of high concentration of silanol groups, which interact with drug moiety through hydrogen bonding in the mesoporous can control the pore size and the surface properties [7,8].

Ordered mesoporous silicates possess a high pore volume that is usually close to 1 cm^3/g, very homogeneous in size, which offers the possibility of embedding many therapeutic agents in a controlled manner. They can be prepared using a combination of self-assembly and sol-gel process, which involves hydrolysis that can be either acid-catalyzed or base-catalyzed (eqn. 1), followed by condensation of silanol as illustrated in eqn. 2 [9]:

$$Si(OR)_4 + 4H_2O \rightleftharpoons Si(OH)_4 + 4R\text{-}OH \quad (1)$$

$$nSi(OH)_4 \rightleftharpoons nSiO_2 + 2nH_2O \quad (2)$$

Ordered mesoporous materials can be synthesized under different conditions such as temperature, time, pH and different directing agents such as silica source [tetraethyl orthosilicate (TEOS), tetramethyl orthosilicate (TMOS) or tetrabutyl orthosilicate (TBOS)] [10] and cationic surfactant such as hexadecyltrimethylamonium bromide [11].

MCM-48 is one of the common mesoporous material that have been used as a carrier for different drugs delivery such as ibuprofen and erythromycin [12,13], cilostazol [14], doxorubicin [15,16], vancomycin [17], camptothecin [18], erythromycin [19], naproxen [20] and valsartan [21]. Drug loading into mesoporous silica can be done by two main approaches (i) solvent-free method in which the drug and the polymer were physically mixed followed by heating to melt, co-milling between the drug and mesoporous materials, and using supercritical carbon dioxide [22]; and (ii) the other approach is solvent-based methods in which the drug is simply dissolved in a suitable solvent, like ethanol then mixed/impregnated with mesoporous silica, followed by appropriate drying techniques at the end of the process [23].

Valsartan, (*S*)-3-methyl-2-(*N*-{[2′-(2*H*-1,2,3,4-tetrazol-5-yl)biphenyl-4-yl] methyl}pentanamido)butanoic acid, is an anti-hypertensive drug. It belongs to family of angiotensin II type I receptor antagonists [24-27]. The absolute bioavailability of valsartan was relatively 23% [28] and undergoes extensive hepatic first pass metabolism. In fact, as shown in Fig. 1, valsartan has two proton dissociating groups; a carboxyl group (pK_a = 3.9) and a tetrazole (pK_a = 4.73) and thus may led to low solubility in acidic stomach media [21]. Any interaction with these groups may change the solubility, the dissolution rate and consequently, the drug release. Many promising formulations were attempted to increase its solubility and control its release using different structured lipid carrier; a blend of lipidic excipients, surfactants and co-surfactants that was composed of 40% w/w water, 10% w/w oleic acid: Labrasol® at a ratio of 2 : 1 v/v and 50% w/w polysorbate 20: Transcutol®-P at a ratio of 1:3 v/v [29], a mixture of compitrol 888 ATO with pluronic F-127 as surfactant using solvent injection method [30], a mixture of long fatty chain triestearin with Capmul MCM and pluronic F-68 using melt emulsification method [31] and a surface modified mixture of Pluronic P123 and teraethylorthosilicate (TEOS) with trimethylbenzene as structure directing agent, the surface modification was done using aminopropyl groups and eudragit L-100-55 [27]. However, they still suffer from simplicity, low-cost and time consuming method by reducing the time and solvent consumption.

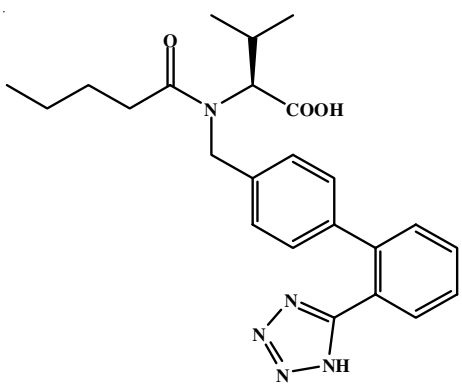

Fig. 1. Chemical structure of valsartan

The objective of this work is to synthesize the mesoporous silicate MCM-48 in a simple (fewer materials and steps), low-cost method and to investigate the impact of drug loading on the release of valsartan from this carrier, aiming to improve the drug solubility and control the drug release. Thermal profiles, FTIR spectra, BET study and particle morphology were also studied to confirm the nature of the drug within the carrier system and the presence or lack of surface crystals. These studies will elucidate the loading efficiency, release behaviour and the nature of the drug within mesoporous carriers.

EXPERIMENTAL

Cetyltrimethylammonium bromide (CTAB) was purchased from Acros Organics, New Jersey, USA, while tetraethylorthosilicate (TEOS) was purchased from Aldrich, St. Louis, USA. Valsartan was kindly supplied by Pharma International, Jordan. Sodium hydroxide pellets (BDH, London), hydrochloric acid 35% (SD Fine-Chem Ltd., Mumbai, India) and absolute ethanol 99.8% (AZ Chem, Pretoria, South Africa) were used as received. Nitric acid 95% (Merck, USA) was used to clean all glass equipments before use.

Synthesis of mesoporous silicate carrier MCM-48: MCM-48 was prepared according to the literature method [32]. An accurate weight of 8.70 g of CTAB as structure directing agent was added to a solution of NaOH (0.96 g) with constant stirring. As a silica source, 10.50 g of TEOS was added dropwise with vigorous stirring till the addition was completed. The solution was further stirred for 1 h at room temperature, transferred to a Teflon-coated stainless autoclave and heated for three days at 100 ºC. Then the stainless autoclave was allowed to cool to room temperature and the pH of the solution was adjusted to 7.0 using 6 M HCl. The mixture was further heated in the autoclave at 100 ºC for one day. The white solid product was filtered, washed with deionized water (3 × 50 mL) and dried at 110 ºC for 12 h. Finally, it was calcined at 550 ºC for 6 h in air to remove the template [1].

Loading of valsartan in MCM-48: A wetness impregnation procedure was used to load valsartan on/or into the MCM-48. A specific amount of 0.2 g of valsartan was dissolved in a mixture of (25.0 mL) water with different fractions of ethanol (10, 12.5, 30, 50 and 100 mL). Ethanol was used as the loading solvent because it is safe, non-toxic and can dissolve large amounts of valsartan. Then, 0.2 g of MCM-48 was added to a flask. After that the mixture was stirred in the dark at room temperature for 24 h to achieve maximum drug loading in the MCM-48 pore channels. Finally, the drug-loaded carrier was filtered and dried under vacuum (30 mm Hg) for 6 h at 25 ºC to remove the solvent completely.

Drug assay

Selection of solvent: The solubility of valsartan in different type of solvents is determined as per Pharmacopeia standard.

Solubility test was done in various solvents like distilled water, methanol, ethanol, 0.1 N NaOH. It was found that from the solubility studies that valsartan is soluble in distilled water, methanol and 0.1 N NaOH. In this study, methanol and distilled water (50:50) were chosen as solvent system.

The concentration of valsartan was determined using UV-visible spectrophotometry at wavelength of 250 nm. The working standard solutions were prepared immediately before use by suitable dilutions of 500 µg/mL stock solution to appropriate concentration levels (5, 10, 20, 30, 40, 50 µg/ mL) by diluting (0.05, 0.1, 0.2, 0.3, 0.4, 0.5 mL) of the stock solution up to 10 mL using volumetric flask. Calibration curve was constructed by plotting the absorbance of the working standard solutions of the drug as a function of the concentration and the regression equations were calculated.

Determination of drug loading: The drug-loaded capacity was determined by the ultraviolet-visible spectrophotometric method. A weight of 10 mg of valsartan loaded MCM-48 (1:1 ratio) was placed in 100 mL volumetric flask that was filled up to volume with solvent system. The contents were stirred with magnetic stirrer for 24 h at room temperature. After this period, the supernatant was filtered through 0.45 µm PTFE syringe filter. The absorbance of the clear filtrate solution was determined at wavelength of 250 nm after suitable dilution. The concentration of the solubilized valsartan in clear filtrate was determined using the linear equation of Beer-Lambert law. Finally, the concentration obtained was multiplied by the appropriate dilution factor and used to calculate the percentage of drug loading according to eqn 3:

$$\text{Drug loading (\%)} = \frac{\text{Mass of loaded valsartan}}{\text{Mass of MCM-48}} \times 100 \quad (3)$$

Thermogravimetric analysis (TGA): Thermal studies of valsartan, MCM-48 and drug loaded carrier were conducted using a Netzsch Sta 409 PC instrument (NETZSCH-Ger) at the temperature range of 25-1000 ºC at a heating rate of 20 ºC/min.

Powder X-ray diffraction (PXRD) analysis: PXRD spectra of valsartan, MCM-48 and drug loaded carrier were obtained using XRD-7000 Shimadzu diffractometer (CuKα radiation source at λ = 1.5418 Å) at a scan rate of 2º/min.

FT-IR analysis: FT-IR spectra of valsartan, MCM-48, and drug loaded carrier in the range from 4000 to 400 cm^{-1}, with 4 cm^{-1} spectral resolution using potassium bromide pellets were measured using a Thermo-Nicolt NEXUS 670 FT-IR spectrometer.

Brunauer-Emmett-Teller (BET) analysis: Specific surface area of mesoporous silica carrier MCM-48 was estimated through BET modelling using a nitrogen adsorption/desorption instrument (Nova 2200e).

SEM analysis: The morphologies of the MCM-48 solid samples were characterized by scanning electron microscopy (SEM) using FEI-FEG INSPEC F50 instrument.

***in vitro* Drug release:** Specific amounts of the valsartan alone (as control) and valsartan loaded MCM-48 (150 mg of dried powder) were compressed using hydraulic press in 9 mm size. Dissolution test of valsartan disks and valsartan loaded MCM-48 disks were carried out in 1000 mL of phosphate buffer (pH 6.8) using USP type II (Paddle type) at a speed of 50 rpm and a temperature of 37 ºC. A sample of 5.0 mL was withdrawn at different time intervals of 5, 10, 15, 20, 25, 30, 60, 90, 120, 150, 180 and 240 min. A fresh medium of 5.0 mL was used to replace the withdrawn sample at each sampling interval. Ultraviolet visible spectrophotometry at 250 nm was used for monitoring the amount of valsartan delivered as a function of time.

RESULTS AND DISCUSSION

Synthesis of mesoporous carriers MCM-48: Mesoporous silicate MCM-48 particulates were prepared using self-assembly method. A typical synthesis of MCM-48 required a minimum of four reagents: a solvent, a silica precursor, an ionic (anionic or cationic) or non-charged surfactant and a catalyst. Depending on the protocol, the reaction could occur in an acidic or basic medium, with different silica/surfactant ratios [33]. In this study, the synthesis was done in alkaline media using TEOS as silica source, CTAB as cationic soft surfactant template, and water and/or ethanol as a solvent. Ethanol was used to decrease the hydrolysis rate of TEOS and reduce the polarity of aqueous solution. Calcination was used as the method for removing the surfactant.

Loading of valsartan into MCM-48: There are various factors that influence the drug loading into mesoporous silica, such as type of solvent, drug load, accessible surface area, and the pore volume of the mesoporous silica. Solvent-based method was used to load valsartan into the mesoporous silicate MCM-48. It was conducted using water and methanol same portion, to optimize the maximum loading of drug in the carrier. Although solvent-free method has lower environmental impact with no need for checking the residual solvent in the final product, solvent based method is more practical and straight-forward solution for drug amorphization within mesoporous silica. In general, solvent-based loading techniques produce drug-loaded mesoporous silica with a high loading efficiency compared to solvent-free techniques [22]. The use of water: methanol same ratio as the loading solvent mixtures have been chosen to meet two goals *i.e.* (i) to enhance the drug solubility, and (ii) to achieve the maximum loading percentage.

The drug loaded capacity was measured using UV-visible spectrophotometer method and confirmed by the TGA and XRD analysis. The concentration of the solubilized valsartan in clear filtrate was determined using Beer-Lambert law. The concentration was 2.006 µg/mL using the line equation of the standard calibration curve ($y = 0.01674x$; $R^2 = 0.999$) over the range of (5-50) µg/mL. Percentage of drug loading according to eqn 3 after multiplying the concentration by the appropriate dilution factor and the final volume was calculated as follows:

$$\text{Drug loading (\%)} = \frac{2006\ \mu g}{5000\ \mu g} \times 100 = 40.12\%$$

Thermal studies: Fig. 2 shows the presence of two main stages of weight loss of MCM-48. The first stage represents desorption of the water molecules that are hydrogen-bonded to the surface silanol groups and water bulk molecules occupy-

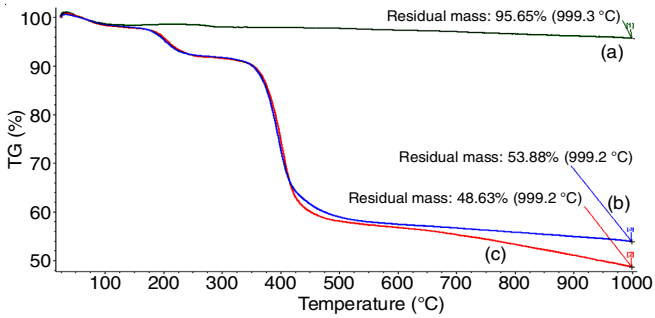

Fig. 2. TGA of (a) MCM-48 (b) VAL (c) drug loaded carrier (12.5% ethanol)

ing within the pores, which took place around 25-200 ºC. The second stage of the weight loss is attributed to the thermal dehydration of surface silanol groups at approximately (300-1000 ºC) [34].

Approximate loading was confirmed by TGA and showed three mass loss regions. The first loss occurred between 60-90 ºC (1-3%) and it is most probably due to the loss of adsorbed water. The second and third losses occurred between 160-300 ºC (13.6 %) and 300-580 ºC (76.6%) and could be due to thermal decomposition of valsartan [35]. The residual mass left at 1000 ºC was about 48.63%; which is due to the presence of thermal stable carrier.

Thermal analysis of valsartan loaded MCM-48 using different fractions of ethanol was also investigated. The percentages of residual mass of the loaded MCM-48 for mixtures of water (25 mL) with different fractions of ethanol *viz*. 10, 12.5, 30, 50 and 100 mL were 41.12, 46.37, 8.44, 7.28 and 7.25%, respectively. The maximum residual mass of the loaded MCM-48 was obtained using a mixture of water (25 mL) with 12.5 mL ethanol.

Powder-XRD studies: Fig. 3 shows the diffraction spectrum of the prepared mesoporous material MCM-48. It shows the highest peak at 2θ of 1.9º and low intensity peaks at 2θ of 2.6º and 2.8º. The pattern is in good agreement with a previous literature data [36].

PXRD spectrum of valsartan shows intrinsic peaks at 5.1º, 11.6º, 15.8º, 18.6º and 26.2 ± 0.2º at 2θ. They indicated the crystallinity of valsartan. Analysis of valsartan loaded MCM-48 spectrum confirmed that valsartan loading with distinctive peak appearance at 2θ of 26º. This is an indication of valsartan crystallization in the pores of the carriers. However, the remarkable weakened crystalline distinctive peaks of valsartan indicated the less ordered crystallinity, rather than completely amorphous state. It indicated a decrease in crystallinity, and transformation into amorphous state. Previous studies [37] showed that higher drug loadings above 30% (w/w) could lead to incomplete amorphization, *i.e*., a small amount of crystalline drug could remain on the exterior surface of the generated particles. Drug molecules can theoretically be adsorbed onto the silica surface of mesopores as a monolayer or multilayers, depending on the drug's molecular dimension, accessible surface area and pore size.

FTIR studies: To explicate the interaction between the MCM-48 and valsartan, FTIR was recorded for valsartan, MCM-48 and the loaded carrier as shown in Fig. 4. It shows distinctive

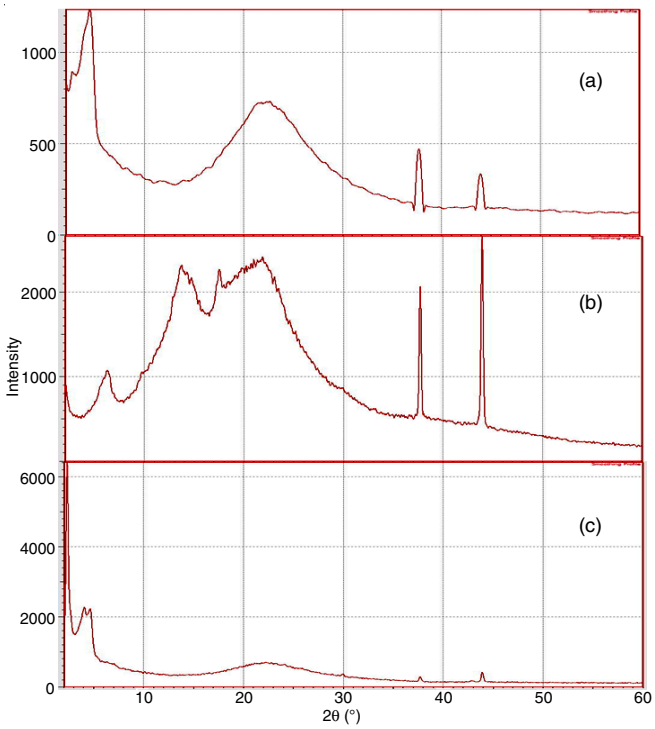

Fig. 3. PXRD spectra of the (a) mesoporous MCM-48 (b) valsartan (c) drug loaded carrier

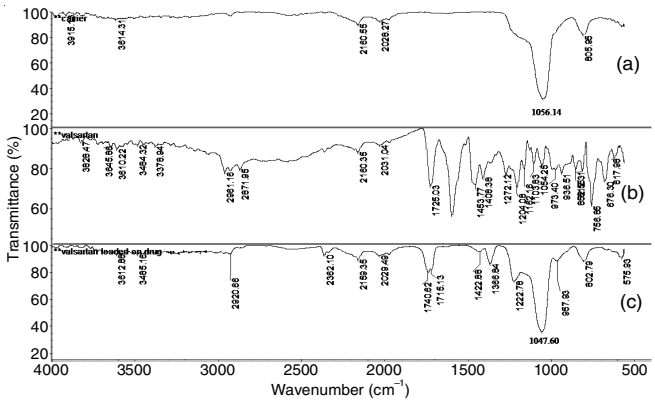

Fig. 4. Infrared spectra of (a) MCM-48, (b) valsartan and (c) drug loaded carrier

characteristic bands of MCM-48 and are consistent with the literature reported data [38]. The corresponding bands assignments are listed in Table-1.

TABLE-1
INFRARED FREQUENCIES OF THE CHARACTERISTIC BANDS OF MCM-48

Group vibrations	Wavenumber (cm^{-1})
ν Si-O-H (free surface)	3915.13
ν Hydrogen-bonds of Si-O-H + ν water	3614.31
Si-O-Si (internal) + ν SiO_4 (asymmetric)	1056.14
Si-O-Si (internal) + ν SiO_4 (symmetric)	805.96

Loading of valsartan into mesoporous carrier was supported by the FTIR analysis. Table-2 shows clearly the presence of valsartan in the loaded MCM-48 samples. Valsartan showed

TABLE-2
INFRARED FREQUENCIES OF CHARACTERISTIC BANDS OF VAL AND VAL LOADED MCM-48

Group vibrations	Wavenumber (cm^{-1})	
	Valsartan	Valsartan loaded MCM-48
O-H and / N-H	3484.32	3485.16
C=O	1725.03	1740.62-1715.13
C–O	1453.77	1422.88
C–N	1054.25	1047.60
C=N	1617.00	Not observed

characteristic sharp, strong bands at 3484 cm^{-1} due to ν(N-H) and ν(-OH). In addition to carbonyl ν(C=O) stretching at 1725 cm^{-1}, imine band stretching ν(C=N) at 1617 cm^{-1}, ν(C-O) band stretching at 1454 cm^{-1} and a band for ν(C-N) stretching at 1054 cm^{-1} [28]. The disappearance of the ν(C=N) and ν(N-H) peaks of valsartan in the spectrum with the shift of the carbonyl peak to the lower energy suggested intermolecular interactions between the valsartan and the MCM-48. These spectra supported the postulation of hydrogen bond formation between the H- bond acceptor valsartan and the proton donor of MCM-48. This could be attributed due to a physisorption interactions that exists between the drug and the carrier in addition to the surface adsorption, which was previously observed in other systems such as zeolite Y [39] and montmorillonite [17]. The bands at 1725 cm^{-1} were divided into two peaks; one appeared at higher wave number while the other appeared at lower wave number; this suggesting the change in the environment of the carbonyl group which could be due to the break and reform of hydrogen bonding.

Nitrogen adsorption/desorption isotherms: Nitrogen adsorption-desorption isotherms were estimated for the carrier MCM-48. The average pore diameter was measured from the desorption branch using the Barrett-Joyner-Halenda (BJH) theory. The specific surface area (A) was measured from the adsorption branch using the Brunauer-Emmett-Teller (BET) theory. The surface area was estimated to be 940 m^2/g (slope = 5.123, intercept = 0.074, R^2 = 0.999). The pore volume and diameter size were 0.6937 cm^3/g and 4.1418 nm, respectively.

Fig. 5 shows the nitrogen adsorption-desorption of the calcined MCM-48. It exhibited a typical type IV curves according to the IUPAC classification of sorption isotherms [40]. It indicated that the pore size of the resulting pore structure was in the range of mesopore with a sharp increment in the adsorption curve up to a relative pressure (P/P_o) of about 0.3. This corresponds to capillary condensation within a regular mesoporous silicate material [32]. The isotherm of the MCM-48 also exhibits the type H1 hysteresis loop associated with the open-ended channel with uniform size and shape.

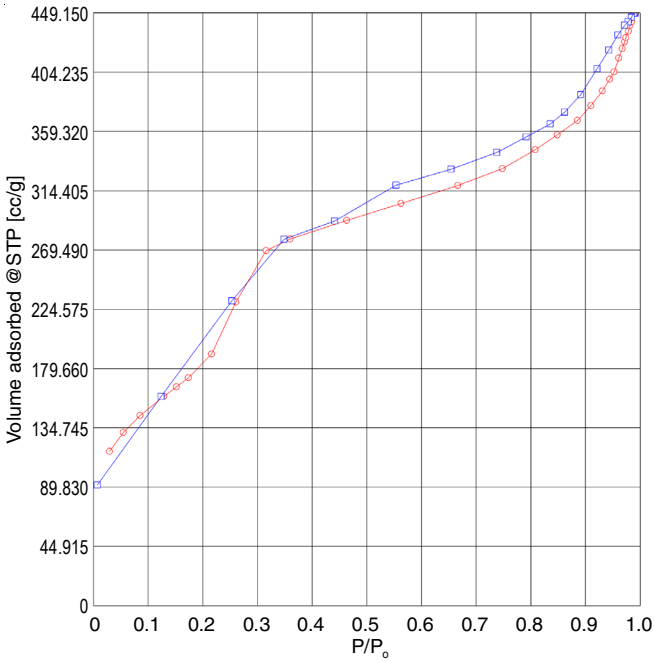

Fig. 5. Nitrogen adsorption/desorption isotherm of MCM-48 (circle points represent adsorption and square points represent desorption isotherm)

SEM studies: Fig. 6 shows the agglomerated uniform spheres with particle size range (152.9-364.2 nm) in the mesoporous silicate MCM-48 morphology, the same is supported by previous study [41].

***in vitro* Drug release studies:** Fig. 7 shows the dissolution profiles of valsartan discs and valsartan loaded MCM-48 discs. Results showed that the dissolution of valsartan loaded MCM-48 samples were much less than that of the valsartan alone ($p < 0.5$). It exhibited a low drug release with only 25% valsartan

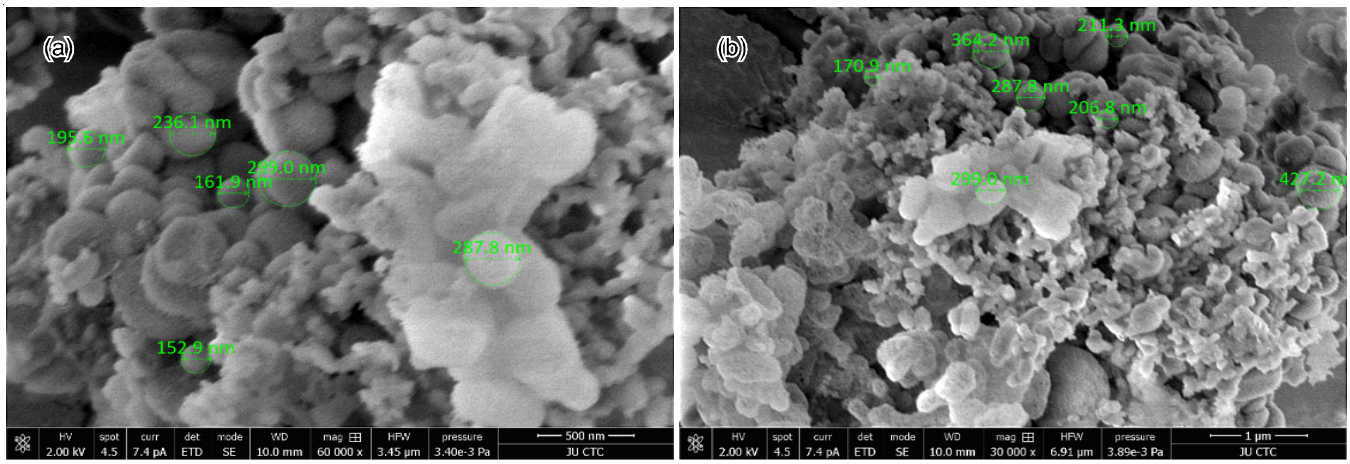

Fig. 6. SEM micrographs of MCM-48 with different power (a) 60000x (b) 30000x

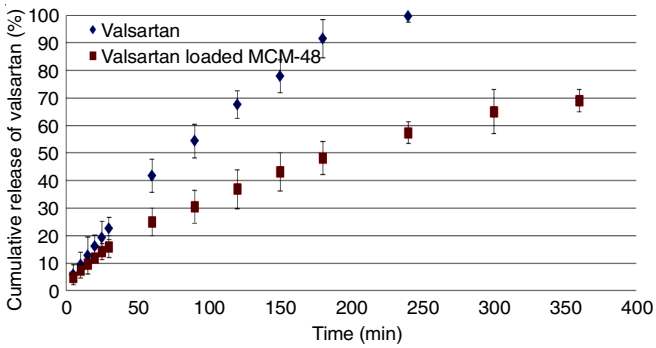

Fig. 7. Cumulative percentage of valsartan released after 240 min from valsartan disks and valsartan loaded MCM-48 using phosphate buffer pH = 6.8 at 37 ± 0.5 ºC (n = 3)

released from the valsartan loaded MCM-48 within the first 60 min, compared to over 42% dissolution from valsartan disk samples. Similarly, after 3 h of dissolution, the percentage of valsartan released from valsartan loaded MCM-48 was 45% compared to 91.5% release from valsartan disk. It is very clear that the dissolution profile of valsartan loaded MCM-48 discs was found to have controlled release compared to valsartan discs with less than 70 % released after 4 h.

To elucidate the underlying mass transport mechanisms and to predict the effect of the carrier parameters (*e.g.*, shape, size and composition of the carrier) on the resulting drug release rate, a well-known semi-empirical power eqn. 4 of Korsmeyer-Peppas was used to analyze the release data:

$$\frac{M_t}{M_\infty} = k\, t^n$$

where M_t/M_∞ is the fractional releasing of the drug; (t) is the releasing time; (k) is a constant characteristic of the drug-carrier system; and (n) is an exponent (release index), which is indicative of the mechanism of the drug release. The value of (n) characterizes the type of release mechanism during the dissolution process. A value of n = 0.5 indicates case I (Fickian) diffusion, 0.5 < n < 1 indicates anomalous (non-Fickian) diffusion and n = 1 indicates case II transport [42].

The estimated value of (n) from the linear regression of log (M_t/M_∞) *versus* log t was found between 0.5 and 1.0, indicating that the release of valsartan is postulated to be non-Fickian diffusion. The obtained values of (k) and (n) were 0.0078 and 0.77, respectively with r^2 (correlation coefficient) value of 0.996. The drug release from this carrier depends on both the interactions between the silica mesopore surface and drug molecules and the diffusion of therapeutic agent molecules through the silica pores.

Thus, the structural properties of mesoporous MCM-48 played very important role in controlling the release of poorly-water soluble valsartan and demonstrated a long-term release, which is important for its antihypertensive activity. In general, mesoporous MCM-48 seems to open new opportunities for controlled delivery system in the near future.

Conclusion

In this study, mesoporous silica MCM-48 was prepared by a facile method using CTAB as template through the introduction of ethanol as a costructure-directing agent. The use of FTIR, nitrogen adsorption/desorption and PXRD confirmed the synthesis of MCM-48 and the effective incorporation of valsartan into the mesopores. The study ascertained the feasibility of developing controlled drug release profile of poorly water soluble valsartan, the reason was attributed to the ordered channels and larger surface area-to-volume ratio of MCM-48. The study of drug release kinetics indicated anomalous (non-Fickian) diffusion. Given the facile synthesis process and excellent drug delivery capacity, mesoporous silica can be considered a good carrier candidate for drug delivery.

CONFLICT OF INTEREST

The authors declare that there is no conflict of interests regarding the publication of this article.

REFERENCES

1. A. Malhis, S. Arar, M. Fayyad and H. Hodali, *Adsorpt. Sci. Technol.*, **36**, 270 (2018); https://doi.org/10.1177/0263617416689270
2. L. Zhang, S. Goh, X. Hu, R. Crawford and A. Yu, *J. Chem. Technol. Biotechnol.*, **87**, 1473 (2012); https://doi.org/10.1002/jctb.3771
3. A. Sayari, *J. Am. Chem. Soc.*, **122**, 6504 (2000); https://doi.org/10.1021/ja0005946
4. C. Bharti, N. Gulati, U. Nagaich and A.K. Pal, *Int. J. Pharm. Investig.*, **5**, 124 (2015); https://doi.org/10.4103/2230-973X.160844
5. B. Zuo, W. Li, X. Wu, S. Wang, Q. Deng and M. Huang, *Chem. Asian J.*, **15**, 1248 (2020); https://doi.org/10.1002/asia.202000045
6. C. Fruijtier-Pölloth, *Toxicology*, **294**, 61 (2012); https://doi.org/10.1016/j.tox.2012.02.001
7. R. Narayan, U.Y. Nayak, A.M. Raichur and S. Garg, *Pharmaceutics*, **10**, 118 (2018); https://doi.org/10.3390/pharmaceutics10030118
8. R. Antoninoa, M. Ruggiero, Z. Song, T.L. Nascimento, E.M. Lima, A.B. Matthias, M. Knopp and K. Löbmann, *Int. J. Pharm.: X*, **1**, 100026 (2019); https://doi.org/10.1016/j.ijpx.2019.100026
9. A.A. Issa and A.S. Luyt, *Polymers*, **11**, 537 (2019); https://doi.org/10.3390/polym11030537
10. D. Arcos and M. Vallet-Regí, *Acta Mater.*, **61**, 890 (2013); https://doi.org/10.1016/j.actamat.2012.10.039
11. M.-S. Kim and I.-H. Baek, *Int. J. Nanomed.*, **9**, 5167 (2014); https://doi.org/10.2147/IJN.S71891
12. I. Izquierdo-Barba, F. Martinez, D. Doadrio, J. P'erez-Pariente and M. Vallet-Regi, *Eur. J. Pharm. Sci.*, **26**, 365 (2005); https://doi.org/10.1016/j.ejps.2005.06.009
13. I. Izquierdo-Barba, E. Sousa, J.C. Doadrio, A.L. Doadrio, J.-P. Pariente, A. Martínez, F. Babonneau and M. Vallet-Regí, *J. Sol-Gel Sci. Technol.*, **50**, 421 (2009); https://doi.org/10.1007/s10971-009-1932-3
14. Y. Wang, L. Sun, T. Jiang, J. Zhang, C. Zhang, C. Sun, Y. Deng, J. Sun and S. Wang, *Drug Dev. Ind. Pharm.*, **40**, 819 (2014); https://doi.org/10.3109/03639045.2013.788013
15. J. Zhang, F. Yuan, Y. Wang, H. Chen, F. Luo, X. Cheng, R.-X. Zhuo and X.-Z. Zhang, *J. Am. Chem. Soc.*, **135**, 5068 (2013); https://doi.org/10.1021/ja312004m
16. V. Mamaeva, M. Rosenholm, T. Bate-Eya, L. Bergman, E. Peuhu, A. Duchanoy, L.E. Fortelius, S. Landor, D.M. Toivola, M. Lindén and C. Sahlgren, *Mol. Ther.*, **19**, 1538 (2011); https://doi.org/10.1038/mt.2011.105
17. C.-Y. Lai, B.G. Trewyn, D.M. Jeftinija, K. Jeftinija, S. Xu, S. Jeftinija and V.S.-Y. Lin, *J. Am. Chem. Soc.*, **125**, 4451 (2003); https://doi.org/10.1021/ja028650l

18. L. Vivero-Escoto, I. Slowing, G. Trewyn and S. Lin, *Small*, **6**, 1952 (2010); https://doi.org/10.1002/smll.200901789
19. M. Gary-Bobo, O. Hocine, D. Brevet, M. Maynadier, L. Raehm, S. Richeter, V. Charasson, B. Loock, A. Morère, P. Maillard, M. Garcia and J.-O. Durand, *Int. J. Pharm.*, **423**, 509 (2012); https://doi.org/10.1016/j.ijpharm.2011.11.045
20. X. Ma, Y. Zhao, W. Ng and Y. Zhao, *Chem. Eur. J.*, **19**, 15593 (2013); https://doi.org/10.1002/chem.201302736
21. D.W. Yeom, B.R. Chae, H.Y. Son, J.H. Kim, J.S. Chae, S.H. Song, D. Oh and Y.W. Choi, *Int. J. Nanomedicine*, **12**, 3533 (2017); https://doi.org/10.2147/IJN.S136599
22. T. Le, A.K.E. Elyafi, A.R. Mohammed and A. Al-Khattawi, *Pharmaceutics*, **11**, 269 (2019); https://doi.org/10.3390%2Fpharmaceutics11060269
23. T. Limnell, H.A. Santos, E. Mäkilä, T. Heikkilä, J. Salonen, D.Y. Murzin, N. Kumar, T. Laaksonen, L. Peltonen and J. Hirvonen, *J. Pharm. Sci.*, **100**, 3294 (2011); https://doi.org/10.1002/jps.22577
24. N.B. Mistry, A.S. Westheim and S.E. Kjeldsen, *Expert Opin. Pharmacother.*, **7**, 575 (2006): https://doi.org/10.1517/14656566.7.5.575
25. A. Markham and K.L. Goa, Drugs, **54**, 299 (1997); https://doi.org/10.2165/00003495-199754020-00009
26. J. Xu, J. Xie, R. Cao, L. Shi, Y. Cao, X.-Y. Zhu and J.-H. Cui, *Drug Deliv.*, **23**, 41 (2016); https://doi.org/10.3109/10717544.2014.903012
27. N. Biswas, *Eur. J. Pharm. Sci.*, **99**, 152 (2017); https://doi.org/10.1016/j.ejps.2016.12.015
28. R. Rajeswari, K. Abbulu, M. Sudhakar, R. Karki and B. Rajkumar, *Der Pharm. Lett.*, **4**, 1044 (2012).
29. R. Abu-Huwaij, R. Hamed, E. Daoud and A. Alkilani, *Acta Pol. Pharm.-Drug Res.*, **76**, 313 (2019); https://doi.org/10.32383/appdr/99526
30. B. Parmar, S. Mandal, C. Petkar, D. Patel and K. Sawant, *Int. J. Pharm. Sci. Nanotech.*, **4**, 3 (2011).
31. R.J. Patel and Z.P. Patel, *Int. J. Pharm. Sci. Nanotechnol.*, **6**, 2077 (2013); https://doi.org/10.37285/ijpsn.2013.6.2.10
32. S. Wang, D. Wu, Y. Sun and B. Zhong, *Mater. Res. Bull.*, **36**, 1717 (2001); https://doi.org/10.1016/S0025-5408(01)00645-6
33. G. Bhattacharyya, G. Lelong and M.-L. Saboungi, *J. Exp. Nanosci.*, **1**, 375 (2016); https://doi.org/10.1080/17458080600812757
34. K. Schumacher, P.I. Ravikovitch, A. Du Chesne, A.V. Neimark and K.K. Unger, *Langmuir*, **16**, 4648 (2000); https://doi.org/10.1021/la991595i
35. M. Skotnicki, P. Cebe and A. Gawel and M. Pyda, *Drug Dev. Ind. Pharm.*, **39**, 1508 (2012); https://doi.org/10.3109/03639045.2012.704379
36. R. Schmidt, M. Stöcker, D. Akporiaye, E.H. Tørstad and A. Olsen, *Micropor. Mater.*, **5**, 1 (1995); https://doi.org/10.1016/0927-6513(95)00030-D
37. W. Xu, H. Xie, Q. Cao, L. Shi, Y. Cao, X.-Y. Zhu and J.-H. Cui, *Drug Deliv.*, **23**, 41 (2016); https://doi.org/10.3109/10717544.2014.903012
38. S. Wu, F. Li, R. Xu, S. Wei and G. Li, *J. Nanopart. Res.*, **12**, 2111 (2010); https://doi.org/10.1007/s11051-009-9770-3
39. A. Datt, A. Burns, A. Dhuna and C. Larsen, *Micropor. Mesopor. Mater.*, **167**, 182 (2013); https://doi.org/10.1016/j.micromeso.2012.09.011
40. K. Sing, *Pure Appl. Chem.*, **54**, 2201 (1982); https://doi.org/10.1351/pac198254112201
41. K. Schumacher, M. Grun and K. Unger, *Micropor. Mesopor. Mater.*, **27**, 201 (1999); https://doi.org/10.1016/S1387-1811(98)00254-6
42. K.E.A. Abou-Aitah, A.A. Farghali, A. Swiderska-Sroda, W. Lojkowski, A.F.M. Razin and M.H. Khedr, *J. Nanomed. Nanotechnol.*, **7**, 351 (2016); https://doi.org/10.4172/2157-7439.1000351